



Passivity based control PBC applied in the buck converter of the stand-alone photovoltaic system

Soltana Guesmi^{1*}, Kais Jamoussi², Larbi Chrifi-Alaoui³, Moez Ghariani², and Kamel Baazouzi⁴

¹ National Engineering school of Sfax ENIS , 3038 SFAX, Tunisia

² National school of Electronics and Telecommunications ENET'Com, 3018 SFAX , Tunisia

³ University of Picardie Jules Verne, Cuffies02880, France

⁴ University of Batna, Algeria

*Corresponding author: soltanaguesmi@gmail.com

Received: 25th February 2019

Revised: 19th October 2019

Accepted: 23rd December 2019

OPEN ACCESS 

Abstract: This paper presents an improved new control technique of the stability of the DC-DC buck converter supplied by a standalone photovoltaic system. The newly designed control based on passivity PBC can stabilize the control system by taking into account the stored energy. The system is modeled under the formalism of Euler Lagrange, to build a passive control law while guaranteeing satisfactory static and dynamic performances. Designed controllers of PBC, photovoltaic panel, and DC-DC buck converter will be simulated using MATLAB/Simulink toolbox and they will be validated by an experimental setup, which ensures the stability and the robustness of the control synthesis in different tests.

Keywords: buck converter, PBC control, Stability, Standalone PV system.

Introduction

Due to population growth, the energy demand has drastically increased. Traditional and old sources of energy cannot meet all demands, thus more researches focused on obtaining alternative and renewable sources of energy are a most. In fact, renewable energy is considered the most effective solution to overcome the energy scarcity and to reduce the damage to the ozone layer in the earth's atmosphere. Solar energy systems as a renewable energy source, ecofriendly for the environment have many advantages for instance; low maintenance, abundance of energy sources, and a zero post-production pollution. Thanks to it, photovoltaic electricity is obtained by directly transforming sunlight into electricity, using photovoltaic cells.

According to my researches [2, 3] and the literature

[4, 5], the external parameters of PV cells (irradiance and temperature) affect the module efficiency and the maximum power extraction. Because of the non-linearity of the I-V and P-V characteristics, the tracking MPP becomes more and more complicated and it becomes a major problem in the photovoltaic sector. To cope with this problem, both of temperature and irradiance shall take a uniform value during the day; and thus, a single MPP. However, when the photovoltaic system is directly connected to the load, the photovoltaic power generation will suffer from disruption because the power output depends on the load's characteristics. To improve the efficiency of the complete system, many researches have proven that adding an algorithm between the photovoltaic system and the load is critical, [6, 7], ensure that the system is operating on its maximum power and under various irradiance conditions. Photovoltaic systems

are generally composed of series and parallel number of photovoltaic modules covering large areas. In some times and due to moving clouds, passing on trees or neighboring buildings, the PV arrays are partially shaded. Under these conditions (PSCs), the power to voltage curve becomes more complex because it is characterized by numerous maximum power point and the power will suffer from disruption. As a result, the efficiency of the system will be reduced and it can supply the load normally [8]. Many control systems are used to reduce the negative effects of climatic condition variation on the photovoltaic system. Firstly, the duty cycle control of the accompanied DC-DC converter by using a classical PI controller. This type of converter doesn't give a good performance in the case of large parameter variations [9] [10]. Secondly, the sliding mode controller SMC; it is a nonlinear control method, which modifies the dynamicity of a nonlinear system by the application of a discontinuous control signal. It is known as the nonlinear robust control compared to the traditional controller system for DC-DC converter control [9- 12]. However, this kind of controller has mains problems such as variation of the switching frequency, the steady-state error and

Materials and Methods

The photovoltaic generator

Figure1 illustrates a global system, consist of a PV system controlled by an effective technique of stability. It consists of two photovoltaic modules of 50W each one, DC-DC converter with MPPT algorithm and resistive load. All PV parameters are presented in Table I. The simulation results of the photovoltaic panel are presented by elaborating on the I-V and P-V characteristics in various values of temperature and irradiance.

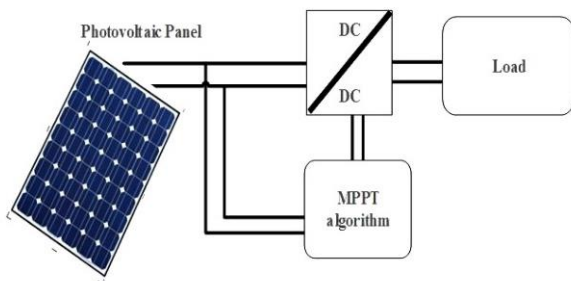


Figure 1. The complete description model of stand-alone photovoltaic system

chattering phenomenon under large variation of DC-DC parameters. To overcome this problem, we seek to improve the performance of parameters, to impose minimum storage energy at the desired point of equilibrium, and to ensure asymptotic stability in the second stage.

A control technique based on passivity PBC will be presented in this paper, it gives them possibility to adjust the duty cycle ratio of the converter, in such a way it will operate at the desired current or voltage. This technique is inspired by Takegaki and Arimoto's works [13] in robot manipulator control, this well-known and highly successful field. The idea gives rise to look for the stability of the mechanical systems, formulated by the equations of Euler Lagrange, and by the formation only of potential energy. This work provides a good validation of the experimental results of the PBC controller in a high-power system established on a stand-alone photovoltaic system based on a PV panel /DC-DC buck converter with resistive load. The test bench is installed in the laboratory of innovative technology.

Table 1. The comparison of alternative journal systems

Description	Value
Open Circuit voltage(V)	22.1
Short Circuit current(A)	3.02
Peak voltage at STC(V)	18.1
Peak current at STC(A)	2.75
Peak Power(W)	50

DC-DC converter and passivity based controller PBC

DC-DC converter model

To manipulate the power transfer between the photovoltaic converter and the load, we need to add an associated switched converter. In our case, and according to the two types of source and load, a DC-DC converter is chosen. The three main types of DC-DC converters used are the Buck Converter, the Boost Converter, and Buck-Boost Converter. In this paper, we opted for the DC-DC buck converter, as schematized in the Figure 2. The mathematical equations for the Buck converter are as indicated in the (1) and (2). From Equation (1), we can deduce that D is the duty ratio of the switch command signal, as a mean parameter of the MPPT controller to extract the maximum possible power of the panel [14].

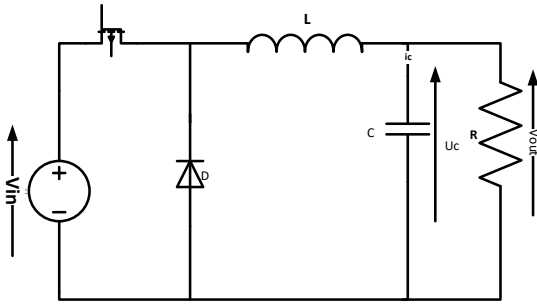


Figure 2. DC-DC Buck converter

$$V_{out} = DV_{in} \tag{1}$$

$$\begin{cases} D = \frac{t_{on}}{t_{on}+t_{off}} \\ t_{on} = DT_s \\ t_{off} = (1 - D)T_s \\ T_s = \frac{1}{f_s} \end{cases} \tag{2}$$

Where, D is the duty cycle of the converter, the subscripts ton and toff are the on-off times respectively, Ts is the switching period and fs is the system frequency. The output voltage is changed by varying the duty cycle. It is used to supply a resistive load under the desired voltage by applying a passive control law PBC. The inductor value is equal to 15mH and the capacitor value is 2200µF.

PBC control

Buck converter design:

In order to supply our load by the desired voltage, the output voltage must suitably follow the reference voltage. The latter can be like the speed or the torque of an asynchronous motor powered by a photovoltaic panel, otherwise, this voltage can be the state of charge SOC of the storage battery of a photovoltaic installation equipped with motorization. A suitable passivity-based control algorithm is applied by modifying the duty cycle of the DC-DC buck converter. The goal of passivity is to converge the trajectories of the system to the desired point of equilibrium at a minimum of energy losses. Besides, passivity-based control PBC aims to render the closed-loop system passive by minimizing the storage energy; in capacitor and inductance. A mathematical model of DC-DC converter based on Euler-Lagrange design will be established as a goal to achieve the strategy of the passivity-based control. The main objective is a dynamic reference tracking performance to minimize the oscillations (in average terms or at the scale of the switching period) parasitic which constitute as much stress on the component or the network to which is connected to the converter.

According to Figure 2, capacitor current is written as follows:

$$i_c = C \frac{dv_c}{dt} = C \frac{dV_{out}}{dt} \tag{3}$$

Where ic, vc, Vout and C are the capacitor current, capacitor voltage, output voltage, and the capacitor value respectively. In our work, we consider that the value of parasitic elements of the inductor, output capacitor and power switches are negligible.

The power switch of the DC-DC Buck converter operates into two states:

ON-state (0<t<DTs), the equivalent circuit of DC-DC converter becomes as indicated in the Figure 3(a):

$$\begin{cases} L \frac{di_l}{dt} = -V_{out} + V_{in} \\ C \frac{dV_{out}}{dt} = i_l - \frac{V_{out}}{R} \end{cases} \tag{4}$$

Considering the input inductor current x1 and the output voltage x2; $i_l = x_1$ and $V_{out} = x_2$

$$\begin{cases} \dot{x}_1 = -\frac{1}{L}x_2 + \frac{1}{L}V_{in} \\ \dot{x}_2 = \frac{1}{C}x_1 - \frac{1}{RC}x_2 \end{cases} \tag{5}$$

OFF-state (DTs <t<Ts), the equivalent circuit of DC-DC converter becomes as shown in Figure 3(b):

$$\begin{cases} L \frac{di_l}{dt} = -V_{out} + v_d \\ C \frac{dV_{out}}{dt} = i_l - \frac{V_{out}}{R} \end{cases} \tag{6}$$

The same as in ON-state, we suppose $i_l = x_1$ and $V_{out} = x_2$

$$\begin{cases} \dot{x}_1 = -\frac{1}{L}x_2 + \frac{1}{L}v_d \\ \dot{x}_2 = \frac{1}{C}x_1 - \frac{1}{RC}x_2 \end{cases} \tag{7}$$

According to the two systems (5) and (7), the DC-DC buck converter can be modeled by the two following equations:

$$\begin{cases} \dot{x}_1 = -\frac{1}{L}x_2 + \frac{1}{L}uV_{in} + \frac{1}{L}(1 - u)v_d \\ \dot{x}_2 = \frac{1}{C}x_1 - \frac{1}{RC}x_2 \end{cases} \tag{8}$$

Where u is the duty cycle defined as below:

$$u(t) = \begin{cases} 1 & \text{for } t_k \leq t < t_k + DT \\ 0 & \text{for } t_k + DT \leq t < t_k + T_s \end{cases} \tag{9}$$

Passivity control design:

To control the passivity of our system, we need to define the Lyapunov function, called also candidate

function, defined as the energy error (the difference between the state and its point of equilibrium), as indicated in the eq.12.

$$V(x) = \frac{1}{2} X^T A X \tag{10}$$

Where $X = \begin{bmatrix} x_1 \\ x_2 \end{bmatrix}$, $A = \begin{bmatrix} L & 0 \\ 0 & C \end{bmatrix}$,

The Lyapunov function is defined as defined by the stored energy in the inductance and the capacitor of our DC-DC converter using the value of the matrix X and A, as shown in the following equation (11).

$$V(x) = \frac{1}{2} L x_1^2 + \frac{1}{2} C x_2^2 \tag{11}$$

The derivative of the lyapunov function can be calculated as:

$$\dot{V}(x) = L x_1 \dot{x}_1 + C x_2 \dot{x}_2 \tag{12}$$

By using the system of equations as represented in (11), the derive of the Lyapunov function is giving as the following equation:

$$\begin{aligned} \dot{V}(x) &= uV_{in}x_1 - \left[\frac{1}{R} x_2^2 - (1-u)v_d \right] < uV_{in}x_1 \\ \Leftrightarrow \dot{V}(x) &< uV_{in}x_1 \end{aligned} \tag{13}$$

Based on [15] and looking for the definition of system passivity, we can deduce that the buck DC-DC converter is strictly passive. There, the system of its model is represented by the function V, negative definite, that checks the inequality $\dot{V}(x) < uV_{in}x_1$. An averaged model as indicated in the following matrix can describe its model:

$$A \dot{x} + (J + R)x = \mu \tag{14}$$

Where J, R, and μ are constants matrix represented, respectively, as follows:

$$\begin{aligned} J &= \begin{bmatrix} 0 & 1 \\ -1 & C \end{bmatrix}, R = \begin{bmatrix} 0 & 0 \\ 0 & \frac{1}{R} \end{bmatrix} \text{ and } \mu = \\ &\begin{bmatrix} DV_{in} - (1-D)v_d \\ 0 \end{bmatrix} \end{aligned} \tag{15}$$

The error, e (t), is defined as $e(t) = x - x_d$ then equation 14 becomes as follows (16):

$$D\dot{e} + (J + R)e(t) = \mu - [D\dot{x}_d + (J + R)x_d + R_i e(t)] \tag{16}$$

In the second operation, the energy regulation of the system is achieved by:

$$\mu - [D\dot{x}_d + (J + R)x_d + R_i e(t)] = 0 \implies$$

$$\begin{cases} uE = Lx_{1d} + x_{2d} + (1-u)v_d + R_i (x_{1d} - x_1) \\ Cx_{2d} - x_{1d} + \frac{1}{R}x_{2d} = 0 \\ e(t) = [e1 \quad e2] = [x_{1d} - x_1 \quad x_{2d} - x_2] \end{cases} \tag{17}$$

Stability design:

The stability of the system can be assessed by the Lyapunov function. When V(e) is definite negative, as seems in (21), the stability of our system becomes good established according to [16].

$$V(e) = \frac{1}{2} e^T D e \tag{18}$$

The derivative of the Lyapunov function is indicated in the following equation:

$$\dot{V}(e) = \frac{1}{2} \dot{e}^T D e + \frac{1}{2} e^T D \dot{e} \tag{19}$$

$$\text{Where: } \dot{V}(e) = \frac{-1}{2} \left[R_i e_1^2 + \frac{1}{R} e_2^2 \right] < 0 \tag{20}$$

This type of nonlinear controller is used as an ideal model of the converter, without the parasitic element, and to prove its stability, we need to consider its Lyapunov theorem as illustrated in the eq.23. Passive control is used to stabilize a system characterized by more degrees of freedom and control, which used in the context of adaptive control by rendering the system passive [18]. In our case, the passivity is used to regulate the output voltage of a static converter according to the selected reference in the shelter to supply a resistive load. This technique serves the overall stability of the system. This passivity property is integral to many other physical applications such as electrical and electromechanical [18].

PI controller

A Proportional Integral PI controller is a control loop A Proportional Integral PI controller is a control loop feedback mechanism. It is essentially used in more than 95% of closed-loop industrial processes. The PI controller is deployed to correct the error between the desired process variable and the measured one to produce a corrective action mainly used for adjusting the process. Indeed, the performance of the output response of the process is globally influenced by the two PI parameters, the Proportional (P), and the Integral (I) values. We are using a PI controller to improve the evolution of the voltage and peak power of the photovoltaic system. Under a change in the PI controller gain, the value of the output will change. Therefore, the value parameters, Kp and Ki, are achieved by setting Kp= 0.08 and Ki= 0.5 when obtains an optimum response of the output voltage. The

output response of PI controller is represented as follows in the (21):

$$u(t) = K_p e(t) + K_i \int e(t) dt \tag{21}$$

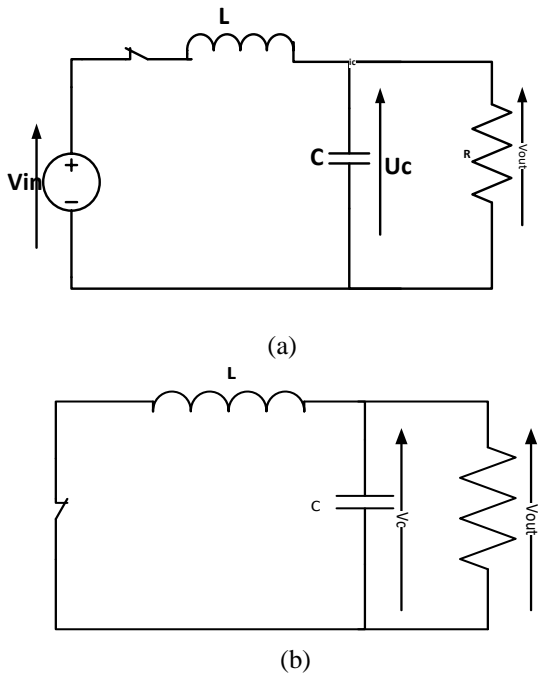


Figure 3. Equivalent circuit of DC-DC buck converter: (a) when switch is ON (b) when switch is OFF

Experimental Validation

In the test of the performance of the proposed PBC algorithm, we employed a Dspace-MicroAutoBox as a controller in the test bench for generating the switch command to the buck DC-DC converter. It is based on a TMS320F240 DSP microcontroller; when, its main function is the management of digital/analog input/output [19]. The algorithm code of the control PBC is generated in Matlab-Simulink by taking input from the controller board CLP1104 DSP and generates output to the same controller board as indicated in the following figure, Figure 4. Besides, its mains input and output are shown in a simple Controlled Desk which facilitates easy communication between MATLAB and onboard DSP. Depending on this, we add sensors to measure the PV voltage, PV current and load voltage, which are inputs signals to the control system as indicated in the Figure 5. Intending to measure the inputs signals by eliminating the high-frequency noise, we add Low pass filters. The PWM command is applied to the switch of DC-DC converter by introducing a DS1104-DSP-PWM block to generate standard 20 kHz fixed-frequency PWM pulses.

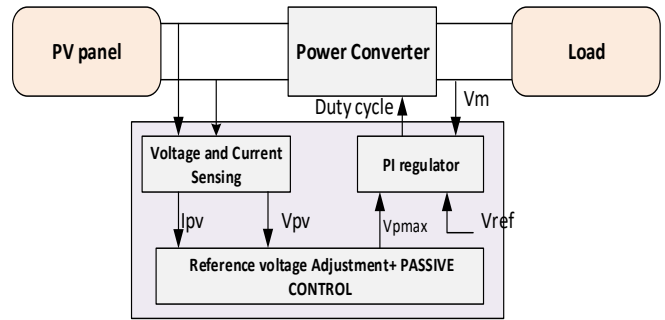


Figure 4. PV panel connected to the load through MPPT algorithm and reference voltage adjustment

Figure 8 clarifies a simple real-time implementation of a PBC controller using a fast dSPACE DSP controller. The system consists of an acquisition model of input/output voltage and current (I_L , I_{ch} , V_{pv} and V_m), a block PBC+PI controller, and a treatment block for PWM generates a signal. To validate the PBC control, the proposed algorithm is tested under four different conditions, i.e. sunny weather ($G=1000W/m^2$), partial shade, total shaded and using another load resistive. We opted to choose a reference voltage that stepped up from $V_{ref}=4.5V$ to $V_{ref}=12V$ at $t=7.5s$, then it changed to another value ($V_{ref}=16.5V$) at $t=15s$ and it increased 21V at $t=22.5s$. Figure 6 gives a schematic representation of the bloc of the PBC principle with a PID controller.

The experimental configuration we used to realize the performance of the PBC controller is shown schematically in Figure 7. We used a SUNMODULE SW 50 POLY RGA/D of SolarWorld Manufacturer as a renewable source, connected to CLP1104 DSP based on DSP microcontroller. Here, the measurement of the inputs/output currents and voltage is done by LA-25NP and LV-25P current and voltage sensor. An interface is used to provide galvanic isolation to all signals connected to the controller board.

Results and Discussions

Simulations and experimental results obtained by MATLAB/SIMULINK and the test bench is shown in figures 9, 10, 11, 12, 13, and 14. The steady-state ripple is about 60mV where the steady-state value of 4.5V as indicated in figure 9.

The first experimental test, as indicated in Figure 10, is done in sunny weather with an equal irradiance of 1000 W/m^2 and temperature equal to 25°C. In this state, the output voltage of the converter suitably follows its reference with a very good performance and without oscillations in both cases of simulation and experimental results.

In the second test, the PV system is partially shaded through the passage of a cloud over part of our photovoltaic panel. The graph of Figure 11 is elaborated when it passes a cloud at the same time, it indicates a similar performance as the case of sunny weather when the reference voltage is inferior to 16.5V but with some oscillation ($V_{ref}=16V$).

In the third test, the PV system is placed under the tree and the irradiance level changes rapidly. The output voltage reaches 17.5V as the maximum voltage of the photovoltaic panel under totally shaded. Under this state, the DC-DC output voltage evolves stably without oscillation and with performance parameters better than the state of partially shaded. These results prove the effectiveness of the proposed controller in terms of stability and performance as indicated in figure 12.

As given in Figure 13 of the fourth test, shows the influence of the load value on the performance and the

stability by assuming the load resistance equals to half of the initial value ($R=250\Omega$). As indicated in the table below, its settling time is two parts less than the case of maximum resistance.

According to the results shown in Table 2, the fourth test has the fastest settling time of 0.24 seconds while the test with 500Ω as a resistance value has the slowest settling time of 0.64 seconds. In addition, for the maximum undershoot, the fourth test with the PBC controller has the best overshoot, which is the lowest one. In contrast, the four tests have the same rise time that indicates the performance parameters of the PBC controller, which is the rapidity of our DC-DC buck converter.

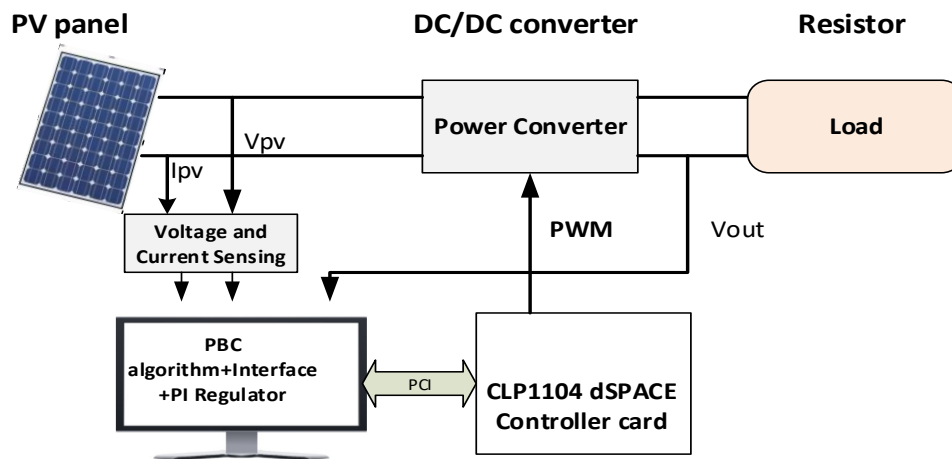


Figure 5. Asymptotic model of experimental test

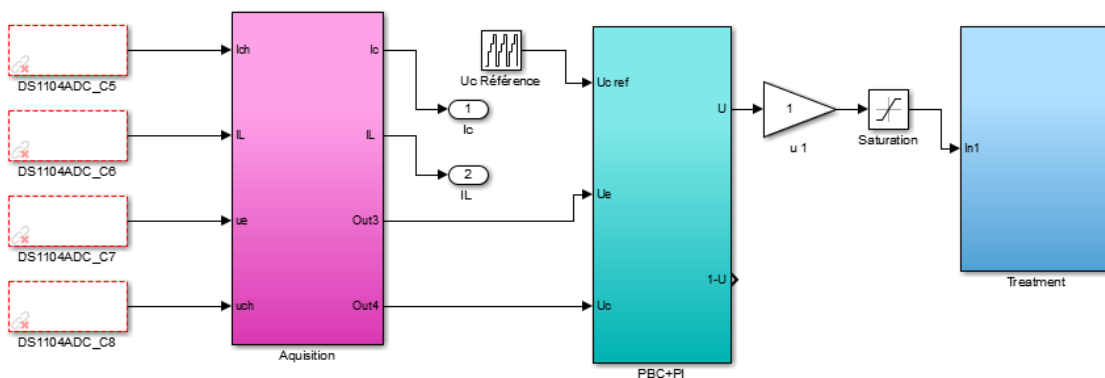


Figure 6. Simulink implementation of PBC controller system with the acquisition bloc

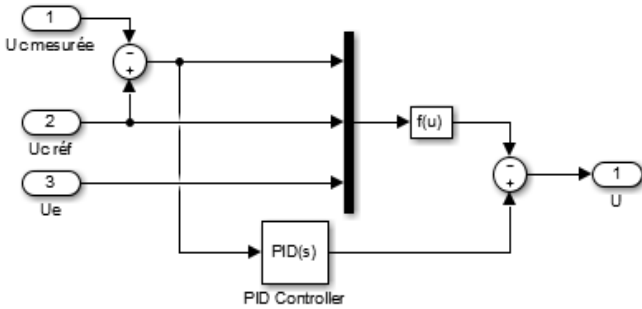


Figure 7. PBC controller with PID regulator

Based on these results, we can conclude that passivity based controller with load value equal to 250 Ω is much better in overall performance including rising time, overshoot, settling time and robustness as compared to the normal condition with resistance value (R=500 Ω). Besides, the experimental and simulation results show that the stability of our DC-DC converter is assured in all tests. As presented in all figures of the four tests (Figure 10, figure 11, Figure 12, and Figure 13), a comparison between the simulated and experimental results have proven the good reliability of our passivity based control.

Table 2. Performance parameters of DC-DC response using PBC control in the four tests:

	Rise time (s) <i>t_m</i>	Settling time(s) <i>t_s</i>	Overshoot	* (s)
1st test	0.1	0.64	5	0.29
2nd test	0.1	0.836	5,5	0.36
3rd test	0.1	0.568	5	0.312
4th test	0.1	0.24	1	0.29

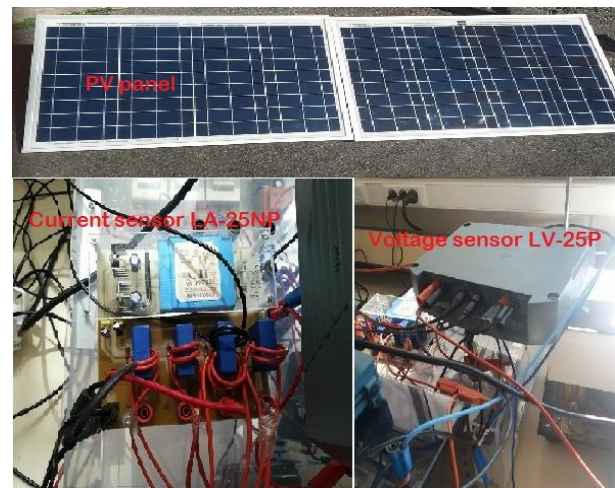
* Steady state establishment time

To make into account the efficiency and the stability of our proposed PBC with PI controller, we are going to compare its response result with the response of a PBC without a PI controller. In Figure 14, the proposed PBC with PI shows a more stable response compared with the one without PI compensator. In fact, its simulation results indicate a null value of the static error.

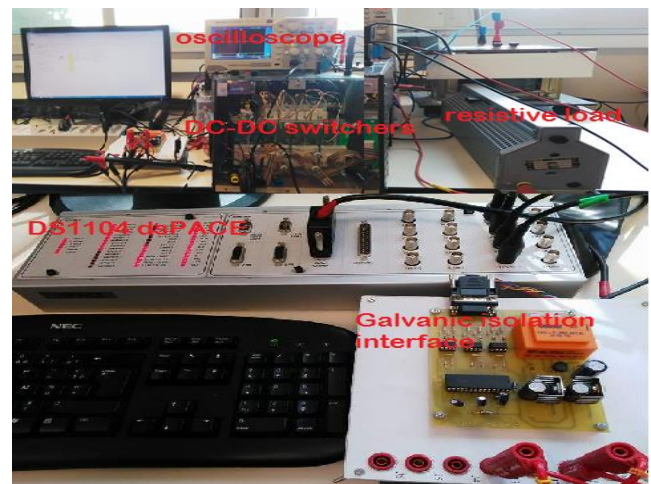
Conclusion

In the work of our developed approach, the passivity-based control is aimed to regulate the output voltage of the DC-DC buck converter supplied by a photovoltaic panel with high power conversion. The developed controller PBC controller in this paper can stabilize converter in high power conversion and large

changes in loads value. The main role of the PBC controller is to manage the energy management between storage energy and supplied energy. This kind of management is formulated by the equations of Euler Lagrange and its simulation results prove the effectiveness of PBC employed in the photovoltaic domain.



(a)



(b)

Figure 8. Experimental test bench: (a) PV panel, current sensor and voltage sensor (b) DC-DC switches resistive load DS1104 DSPACE, Oscilloscope and galvanic isolation interface

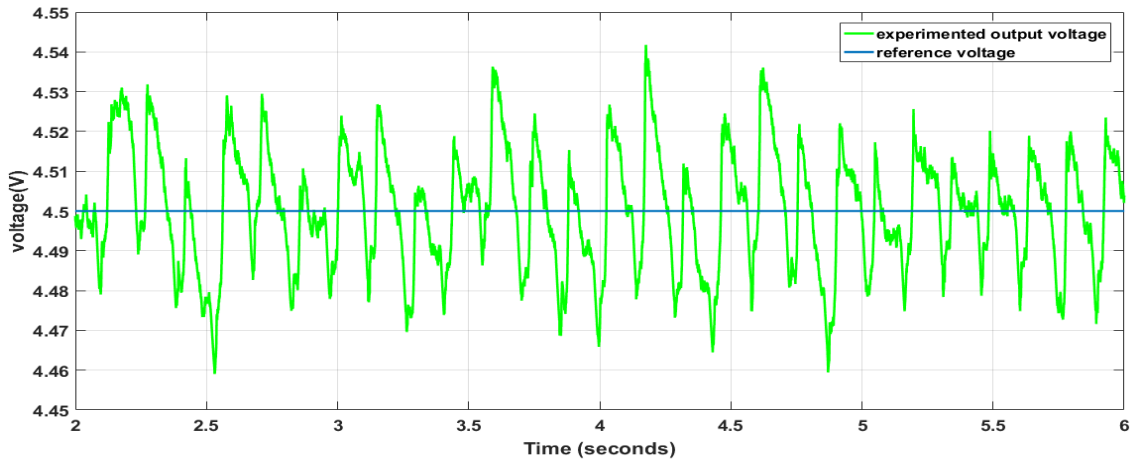


Figure 9. Output voltage ripple

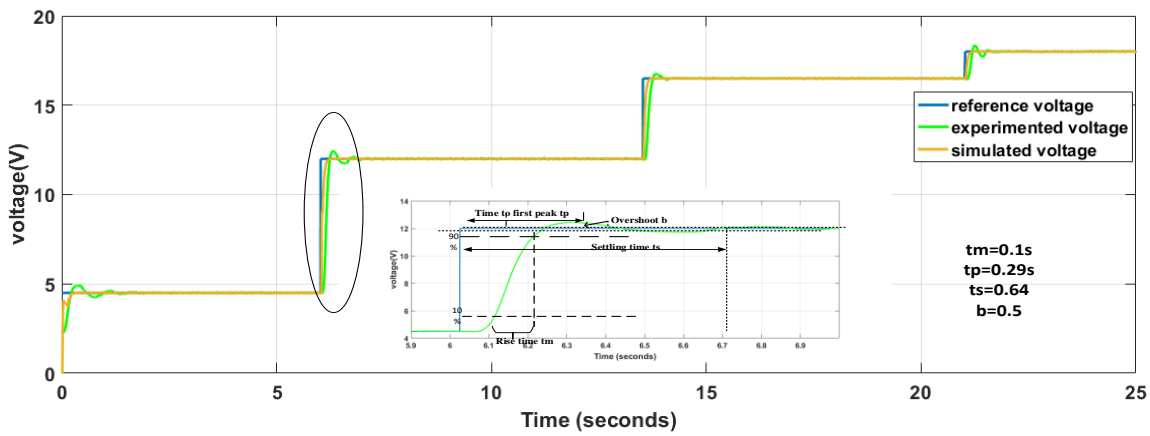


Figure 10. PBC Output voltage control and reference voltage using PBC- test1 at 1000 W/m² (sunny day) and R=500 Ω

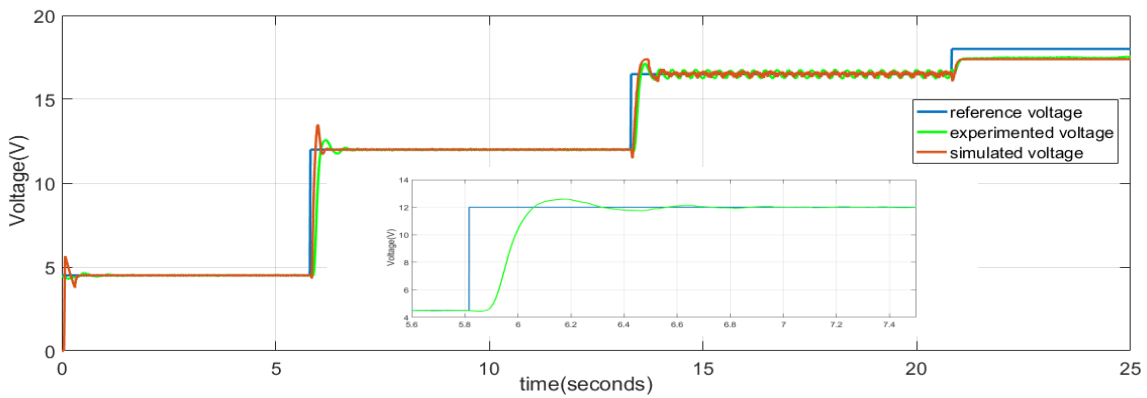


Figure 11. PBC Output voltage control and reference voltage using PBC- test1 in partial shaded (G=50W/m²/T=35°C)

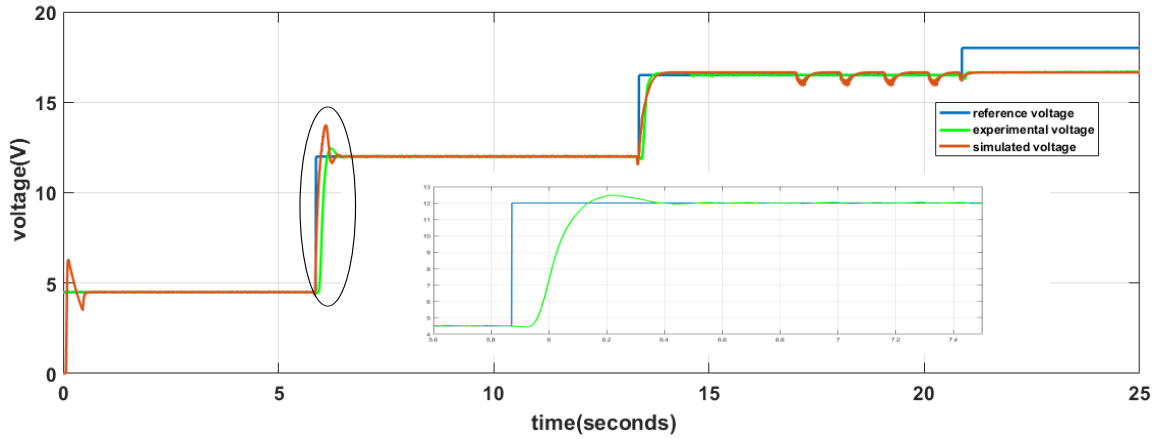


Figure 12. PBC Output voltage control and reference voltage using PBC- test3 in total shaded ($G=33W/m^2$ and $T=17.5^\circ C$)

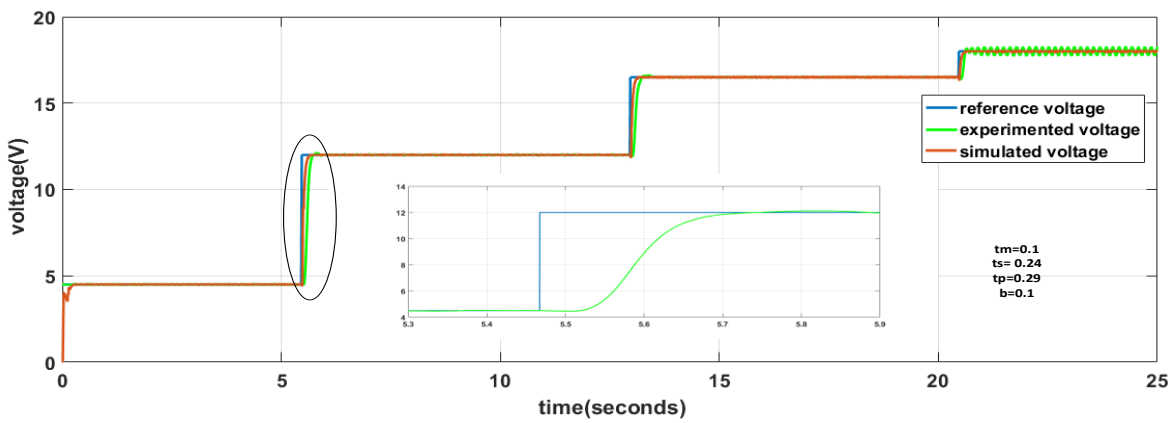


Figure 13. PBC Output voltage control and reference voltage using PBC- test4 at $R=250 \Omega$ at sunny day

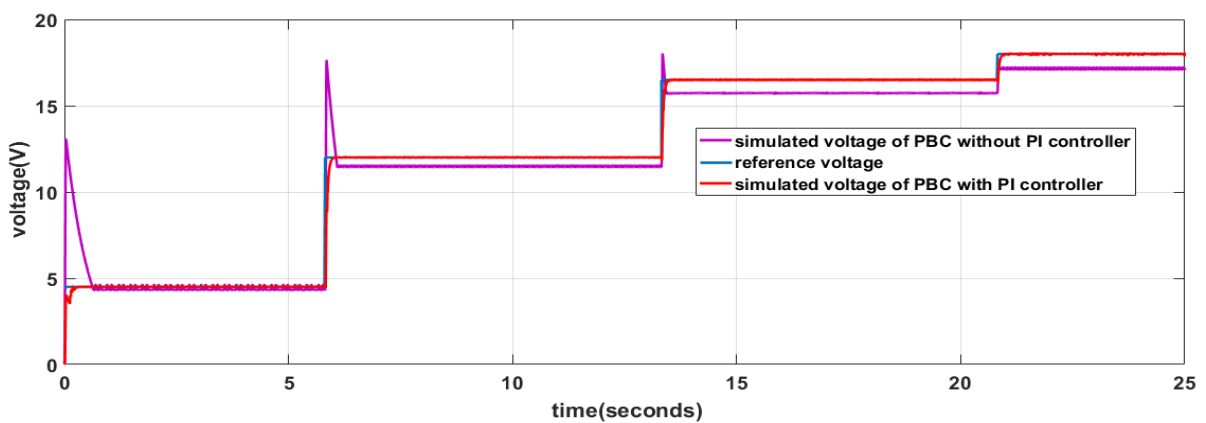


Figure 14. PBC control with and without PI regulator


References

- [1] P. Pudney, and P. Howlett, "Critical speed control of a solar car". Optimization and engineering, vol. 3, no. 2, pp. 97-107, 2002.
<https://doi.org/10.1023/A:1020907101234>
- [2] S. Guesmi, M. Ghariani, M. Ayadi, and R. Neji, "Model of stand-alone photovoltaic module". Proceedings of the International Conference on Recent Advances in Electrical Systems, 2016.
- [3] S. Guesmi, M. Ghariani, M. Ayadi, and R. Neji, "Complete modeling of photovoltaic module with electrical parameters, 2017.
- [4] P. Mahajan, and A. Bhole, "Modeling of photovoltaic module. International Research Journal of Engineering and Technology (IRJET), vol. 2, no. 3, pp. 496-500, 2015.
- [5] C. T. Hsieh, H. T. Yau, C. C. Wang, & Y. S. Hsieh. Nonlinear behavior analysis and control of the atomic force microscope and circuit implementation. Journal of Low Frequency Noise, Vibration and Active Control, 38(3-4), 1576-1593, 2019.
<https://doi.org/10.1177/1461348418775891>
- [6] Y. E. A. Eldahab, N. H. Saad, and A. Zekry, "Enhancing the design of battery charging controllers for photovoltaic systems", Renewable and Sustainable Energy Reviews, vol. 58, pp. 646-655, 2016.
<https://doi.org/10.1016/j.rser.2015.12.061>
- [7] C. T. Hsieh, H. T. Yau, & C. C. Wang. "Control circuit design and chaos analysis in an ultrasonic machining system". Engineering Computations, 34(7), 2189-2211, 2017. <https://doi.org/10.1108/EC-02-2017-0044>
- [8] C. T. Hsieh, H. T. Yau, , C. C. Wang, & Y. S. Hsieh. Particle swarm optimization used with proportional-derivative control to analyze nonlinear behavior in the atomic force microscope. Advances in Mechanical Engineering, 8(9), 1-10, 2016. <https://doi.org/10.1177/1687814016667271>
- [9] K. Jamoussi, M. CHADLI, A. EL HAJJAJI, et al. Robust fuzzy sliding mode observer for sensorless field-oriented control of induction motor. In : 6th International Multi-Conference on Systems, Signals and Devices. IEEE, p. 1-7, 2009. <https://doi.org/10.1109/SSD.2009.4956657>
- [10] S.M. Mahmoud, M. Ouriagli, L. Chrifi-Alaoui, and P. Bussy, "Robust control of nonlinear systems with both matched and unmatched disturbances." in Control & Automation (MED), 18th Mediterranean Conference on. IEEE, 2010, pp. 1043-1048, 2010.
- [11] H. T. Yau, C. C. Wang, C. T. Hsieh, & C. C. Cho. "Nonlinear analysis and control of the uncertain micro-electro-mechanical system by using a fuzzy sliding mode control design ". Computers & Mathematics with Applications, 61(8), 1912-1916, 2011.
<https://doi.org/10.1016/j.camwa.2010.07.019>
- [12] H. T. Yau, C. O. K. Chen, & C. L. Chen. Sliding mode control of chaotic systems with uncertainties. International Journal of Bifurcation and Chaos, 10(05), 1139-1147, 2000.
<https://doi.org/10.1142/S0218127400000803>
- [13] A. Lotfazar, and M. Eghtesad, "Application of passivity based and integrator backstepping control methods on a 5 dof robot manipulator incorporating actuator dynamics. in Automation Congress." Proceedings. World, vol. 15. IEEE, 2004, pp. 185-190, 2004.
- [14] T. N. Nguyen, and A. Luo, "Multifunction converter based on lyapunov function used in a photovoltaic system" Turkish Journal of Electrical Engineering & Computer Sciences, vol. 22, no. 4, pp. 893-908, 2014.
<https://doi.org/10.3906/elk-1210-7>
- [15] M. E. BA, SOGLU and B. Cakir, "An improved incremental conductance based mppt approach for pv modules." Turkish Journal of Electrical Engineering & Computer Sciences, vol. 23, no. 6, pp. 1687-1697, 2015.
<https://doi.org/10.3906/elk-1404-196>
- [16] R. Ortega, J. A. L. Perez, P. J. Nicklasson, and H. J. Sira-Ramirez, "Passivity-based control of Euler-Lagrange systems: mechanical, electrical and electromechanical applications." Springer Science & Business Media, 2013.
- [17] K. Sundareswaran, V. Vigneshkumar, P. Sankar, S. P. Simon, P. S. R. Nayak, and S. Palani, "Development of an improved p&o algorithm assisted through a colony of foraging ants for mppt in pv system." IEEE Transactions on Industrial Informatics, vol. 12, no. 1, pp. 187-200, 2016. <https://doi.org/10.1109/TII.2015.2502428>
- [18] T. Nuchkrua, and T. Leephakpreeda, "Adaptive pid

control of dc-link voltage via dc/dc buck-boost converter. "Science & Technology Asia, vol. 18, no. 2, pp. 42-53, 2013.

[19] T. TMS320LF2407, and D. TMS320LF2402, 1999 Controllers datasheet. Texas Instruments, SPRS0941.

Publisher: Chinese Institute of Automation Engineers (CI.
ISSN: 2223-9766 (Online)

 **Copyright:** The Author(s). This is an open access article distributed under the terms of the [Creative Commons Attribution License \(CC BY 4.0\)](https://creativecommons.org/licenses/by/4.0/), which permits unrestricted use, distribution, and reproduction in any medium, provided the original author and source are cited.